Progress in Organic Coatings xxx (xxxx) xxxx

Contents lists available at ScienceDirect

Progress in Organic Coatings

journal homepage: www.elsevier.com/locate/porgcoat

Evaluation the anti-corrosion behavior, impact resistance, acids and alkali immovability of nonylphenol ethoxylate/TiO_2 hybrid epoxy nanocomposite coating applied on the carbon steel surface

A.M. Fadl[a,*], M.I. Abdou[a], Sultan Abo Al-Elaa[b], M.A. Hamza[c], S.A. Sadeek[d]

[a] Egyptian Petroleum Research Institute (EPRI), Nasr City, Cairo, Egypt
[b] Golden Chemicals Industries Company (Golden Paint), Cairo, Egypt
[c] Chemistry Department, Faculty of Science, Ain-Shams University, Abbassia, Cairo, Egypt
[d] Chemistry Department, Faculty of Science, Zagazig University, Zagazig, Egypt

ARTICLE INFO

Keywords:
Nonylphenol ethoxylate/TiO_2 nanocomposite
Epoxy coating
Anti-corrosion behavior
Impact resistance
Acids and alkali immovability
SEM

ABSTRACT

Nanocomposite modifiers reinforce the whole characteristics of epoxy coatings for different steel surface applications. To support this concept, sol-gel synthesized TiO_2 nanoparticles (TNPs) were mixed with nonylphenol ethoxylate (NPhE) to form nonylphenol ethoxylate/TiO_2 nanocomposite (NPhE/TNC) as a modifier for epoxy coating applied on the C-steel surface. TNPs were characterized by XRD, SEM and HR-TEM techniques. Various modified NPhE/TNC epoxy coating formulations with different loading levels (0.5, 1, 1.5, 2 and 2.5%) by weight were prepared. FT-IR spectra were used for characterizing of the formed nanocomposites. The anti-corrosion behavior of surface-modified NPhE/TNC coated films versus unmodified conventional epoxy was studied by salt spray accelerated corrosion test. The obtained results demonstrated a considerable improvement in the rust grade, blistering size and frequency, and adhesion strength of modified NPhE/TNC epoxy nanocomposite coated films and affirmed by SEM morphology survey. The impact resistances of unmodified and modified NPhE/TNC epoxy coatings were measured where the best impact resistance was recorded for NPhE/TENC-E coated film at 51 J. Acids and alkali chemical immersion test was performed to check the chemical immovability for the surface-modified NPhE/TNC coated films against conventional epoxy where NPhE/TENC-E coating showed the suitable immovability levels.

1. Introduction

Owing to their corrosion mitigation behavior, superior chemical durability, excellent electrical insulation characteristics and remarkable mechanical and thermal properties, epoxy coatings containing nano-fillers have been utilized [1–4]. The ability of epoxy coatings to mitigate the diffusion of aggressive species such as water, oxygen, and chlorides depends on the formed physical barrier film which diminishes the metallic substrate corrosion during the direct exposure to the corrosive media [5]. Epoxy coating deterioration can be observed during the direct exposure to corrosive electrolytes due to the generation of localized defects such as holes, voids, and cracks via the coating layer [6]. With long exposure to the corrosive medium, the depth and width of these defects will increase and the coating layer tends to be fully degraded [7]. The blending of nanoparticles with epoxy resins displays eco-friendly robust emulsions to enhance the integrity and durability of coatings because these particles can occupy free coating spaces established from the curing shrinkage of an epoxy vehicle [8–10] causing enhancement in the cross-linking density [2].

Recently, some studies investigated the enhanced protective behavior of TiO_2/ glycidoxypropyl trimethoxy silane epoxy nanocomposite coating on 2024-T3 aluminum alloy surface by using salt spray and characterized by electrochemical impedance spectroscopy (EIS) methods. The obtained results demonstrated an outstanding barrier film, enhanced pencil hardness and improved glass transition temperature when compared to untreated neat epoxy [11]. It was found that the epoxy coating properties (e.g. abrasion, friction resistances, swelling, water permeability reduction and hardness), were enhanced by dispersing TiO_2 nanoparticles through the epoxy matrix rather than in case of micro-sized grains [12,13]. The anti-corrosion, thermal and surface characteristics of DGEBPA-titania-polyamide (DGE–TiO_2–PA) hybrid coating were investigated. The results revealed a positive improvement and wide application insights of the epoxy hybrid nanocomposite [14]. The influence of TiO_2/silane nanocomposite on the

* Corresponding author.
E-mail address: fadl8693@yahoo.com (A.M. Fadl).

https://doi.org/10.1016/j.porgcoat.2019.105263
Received 12 July 2019; Received in revised form 30 July 2019; Accepted 1 August 2019

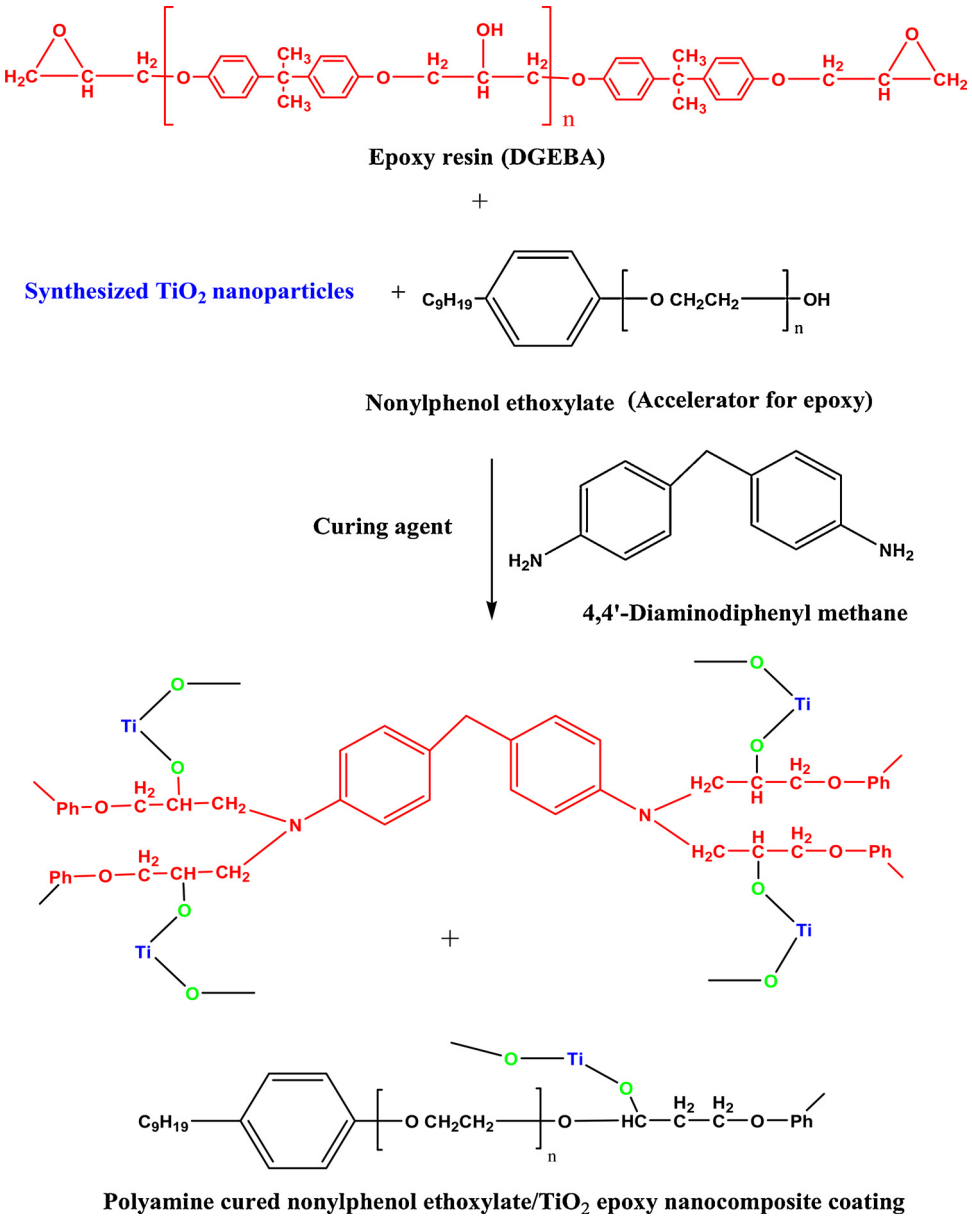

Scheme 1. Formation of cross-linked three-dimensional networks of nonylphenol ethoxylate/TiO_2 epoxy nanocomposite.

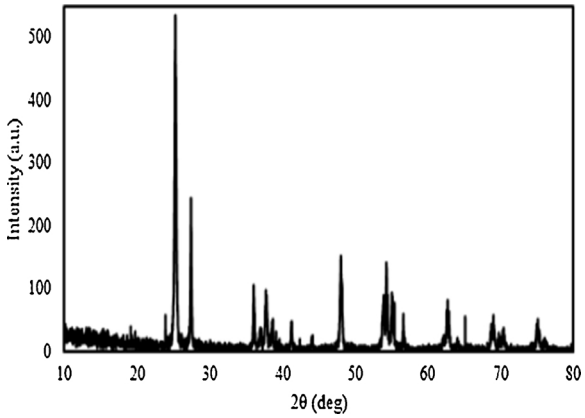

Fig. 1. XRD patterns of the synthesized TiO_2 nanoparticles (TNPs).

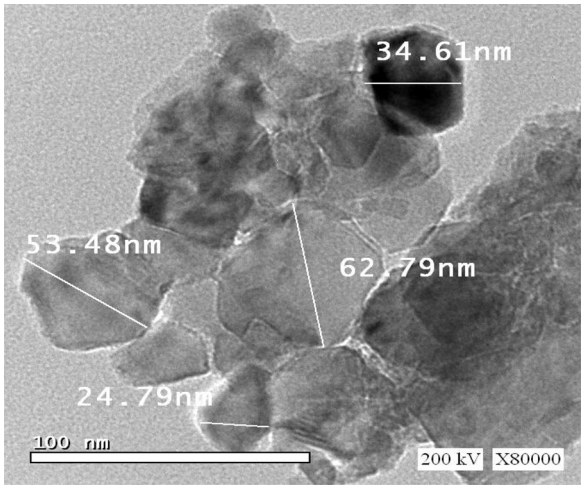

Fig. 2. TEM micrograph of lamellar-shaped TNPs.

corrosion mitigation, mechanical and thermal properties of a bisphenol-A based phthalonitrile resin was also investigated [15].

Nonylphenol ethoxylates (NPhEs) are non-ionic surfactants utilized in a broad range of applications such as detergents, emulsifiers, paints, coatings and emulsion polymerization. NPhE surfactants are utilized for increasing the surface activity and providing excellent solubility.

The present work aims to evaluate the utilization of prepared NPhE/TNC as a modifier to show its effect on enhancing the anti-corrosion behavior, impact resistance and chemical durability of epoxy coating applied on the C-steel surface. The assessment of the surface-modified NPhE/TNC epoxy coatings against conventional epoxy was performed using salt spray, impact, and chemical immersion tests to guarantee their effectiveness in the coating application.

2. Experimental

2.1. Materials

Titanium tetra-isopropoxide ($Ti(OCH(CH_3)_2)_4$) was purchased from Sigma Aldrich, D. E. R 671-X75 (Epoxy vehicle of DGEBPA type) was obtained from Dow Chemical's Co, Ancamine 1734 contains DDM (4,4′-Diaminodiphenyl methane), as a curing agent (hardener), was purchased by Anchor Chemicals Agency. Other chemicals used in this work were of pure grade and used as received without any further purification. The C-steel specimens were prepared with 2 mm x 10 cm x 15 cm dimensions to be used for salt spray test. The coupon dimensions for impact and chemical resistance coating tests were 0.8 mm x 10 cm x 15 cm. Steel coupons were pretreated by sandblasting machine to obtain surface roughness of 30 µm then, washed with acetone and distilled water to be ready for the coating application. The utilized C-steel specimens have chemical composition as illustrated: C 0.160%, Cr 0.5%, Ni 0.063%, Mn 1.650%, P 0.020%, Si 0.450%, S 0.001%, Al 0.043%, Fe Balance.

2.2. Synthesis of TiO_2 nanoparticles

Titanium dioxide nanoparticles (TNPs) were synthesized by a sol-gel method. Typically, 20 mL of $Ti(OCH(CH3)_2)_4$ was dissolved in 200 mL isopropyl alcohol, after 1 h of stirring, few drops of distilled water were added dropwise to hyrolyse the precursur solution to $Ti(OH)_4$ sol. After 2 days of aging, $Ti(OH)_4$ gel was filtered and washed several times with distilled water and isopropanol. Finally, TNPs were obtained after drying at 80 °C for 24 h and calcination at 550 °C for 4 h with a heating rate of 5 °C.min^{-1} [16].

2.3. Characterizations for the synthesized TiO_2 nanoparticles

X-ray diffraction (XRD) paterns were measured using PANanalytical X'pent PRO to investigate the crystal phase of TNPs. Transmission electron microscope (TEM) image was recorded at 200 KV electron microscope model (JEM 2100 LaB6, Japan) with resolution accuracy up to 0.0143 nm. Scanning electron microscopic (SEM) image was clarified by JOEL-5410 scanning electron microscope (Japan) at a magnification of 1000×.

2.4. Preparation of nonylphenol ethoxylate/TiO_2 epoxy nanocomposite formulation coatings

The synthesized TNPs were added to NPhE in different weight percentages (30:70%). Then, isopropyl alcohol and cyclohexanone were added with a vigorous stirring to ensure well dispersion and high homogeneity. The composed mixture was modified with 0.5% of ethylene glycol (EG) and 0.15% of dioctyl phthalate (DOP), then ultrasonicated for 30 min to obtain NPhE/TNC paste. The as-prepared NPhE/TNC paste was anchored on the epoxy resin (DGEBPA), as coating modifier with different loading weight percentages (0.5, 1, 1.5, 2 and 2.5%). Then, xylene and isopropanol were added to the formed coating suspensions and subjected to ultrasonication for 30 min to ensure the full-dispersion of coating constituents. Five treated nanocomposite epoxy coating formulations (NPhE/TENC-A, NPhE/TENC-B, NPhE/TENC-C, NPhE/TENC-D and NPhE/TENC-E) were obtained besides neat epoxy (blank conventional coating). Ancamine 1734 was used as an epoxy curing agent (hardener), and the two parts were mixed as 1:1.65 wt percentages (hardener:epoxy). The cured coating layer (dry film thickness, DFT) on C-steel substrate was gauged in the range of 40 ± 5 µm.

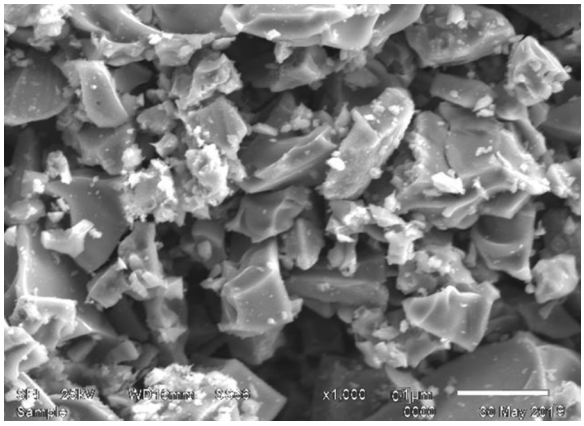

Fig. 3. SEM image of flaky-like shaped TNPs.

2.5. FT-IR spectra

FT-IR spectra for NPhE/TNC paste, surface-modified NPhE/TNC coatings and blank conventional epoxy cured by polyamine curing agent, were analyzed using Nicolet IS-10-FTIR Thermo Fisher spectrophotometer (400-4000 cm^{-1}). The cured coating sample outcomes were fitted with the signals of the background spectrum.

2.6. Salt spray accelerated corrosion experiment

The test procedures were performed using Sheen salt spray chamber (closed system). The coated steel specimens were fixed in parallel plates of the employed chamber with approaching humidity of 95% and 5% NaCl as a test solution at 35°C according to ASTM B117-03. A sharp steel cutter was used to create cross lines in the middle of coated steel specimens to permit the test aggressive fog to penetrate the steel specimens to check the adhesion strength of coating under the coated zone. The test was performed continuously after 500 h of direct exposure to the aggressive fog. The anti-corrosion performance was assessed in the terms of softening grade (API 5L2 4th edition, July 2002), blistering size and frequency (ASTM D 714-02), a degree of rusting (ASTM D 810-01), and adhesion strength class (ASTM D 3359-97).

2.7. Surface morphology investigation of unmodified and modified NPhE/TNC epoxy nanocomposite coated C-steel specimens

The surface morphology of unmodified (neat epoxy) and modified epoxy nanocomposite coated films (NPhE/TENC-A, NPhE/TENC-B, NPhE/TENC-C, NPhE/TENC-D, and NPhE/TENC-E) were evaluated by SEM after direct exposure to the salt spray corrosive fog (5% NaCl solution) for 21 days. All SEM images of the checked coated specimens were clarified by QUANTA FEG 250 scanning electron microscope and implemented at 2000X magnification.

2.8. Impact (resistance to rapid deformation) test

The impact resistance of the coating layer was measured according

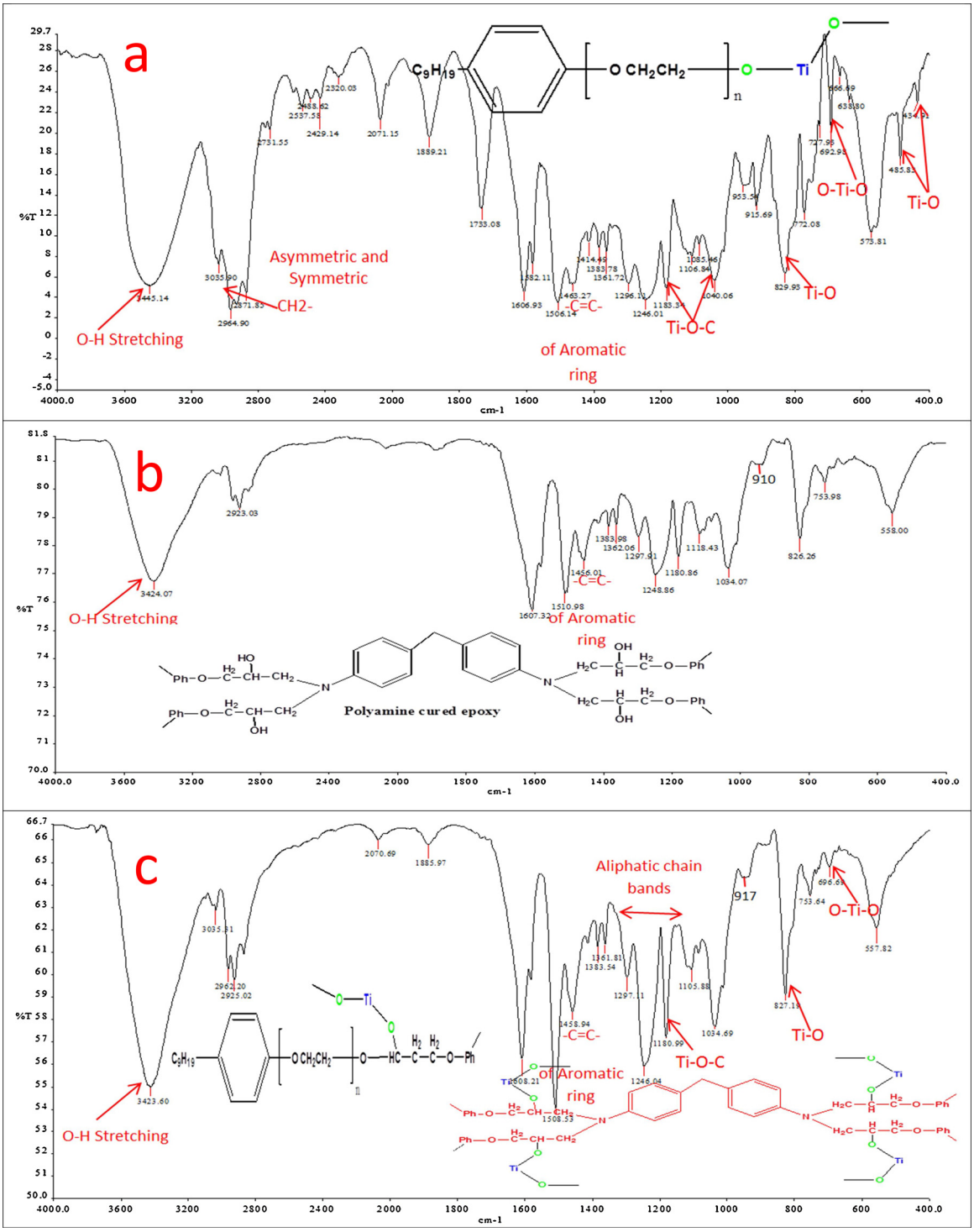

Fig. 4. FT-IR spectra of a) Nonylphenol ethoxylate/TiO_2 nanocomposite (NPhE/TNC) paste, b) Cured conventional epoxy and c) Surface-modified NPhE/TNC cured epoxy layer.

to (ASTM D 2794-93, Reapproved 2019) by utilizing a tubular impact tester. This method has been used to predict the ability of the epoxy layer to resist the cracking caused by impacts. The impact apparatus is consisting of a vertical tube to guide a cylindrical weight that is dropped on a punch resting on the test coated panel. The coatings under test are applied to suitable thin metal panels. After the coatings have cured, a standard weight is dropped a distance so as to strike an indenter that deforms the coating and the substrate. The indentation can be either an intrusion or an extrusion. By gradually increasing the distance the weight drops, the point at which failure usually occurs can be determined. Films generally fail by cracking, which is made more visible by the use of a magnifier, by the application of a copper sulfate ($CuSO_4$) solution on steel, or by the use of a pin holes detector. For each kilogram-meter level, tabulate the number of times the coating passed or failed. The values where the results change from mainly passing to mainly failing is the impact failure end point. An equation was used for calculating the impact values as (the work done on the surface of the coating layer):

$$\text{Impact value (J)} = F \times d = m\ g \times d$$

Table 1
Accelerated corrosion experiment for unmodified and modified NPhE/TNC epoxy coated films after 500 h exposure in salt spray cabinet using 5% NaCl soln.

Adhesion cross-cut	Softening	Rust grades	Blistering		Coating code
			Frequency	Size	
1B	Observed	3	Medium Dense	#3	Blank epoxy coating
3B	Observed	4	Medium	#3	NPhE/TENC-A
3B	Not observed	6	Few	#4	NPhE/TENC-B
4B	Not observed	7	Few	#6	NPhE/TENC-C
5B	Not observed	9	Medium	#8	NPhE/TENC-D
5B	Not observed	10	Few	#8	NPhE/TENC-E

NPhE/TNC: Nonylphenol ethoxylate/TiO_2 nanocomposite.
NPhE/TENC: Nonylphenol ethoxylate/TiO_2 epoxy hybrid nanocomposite.

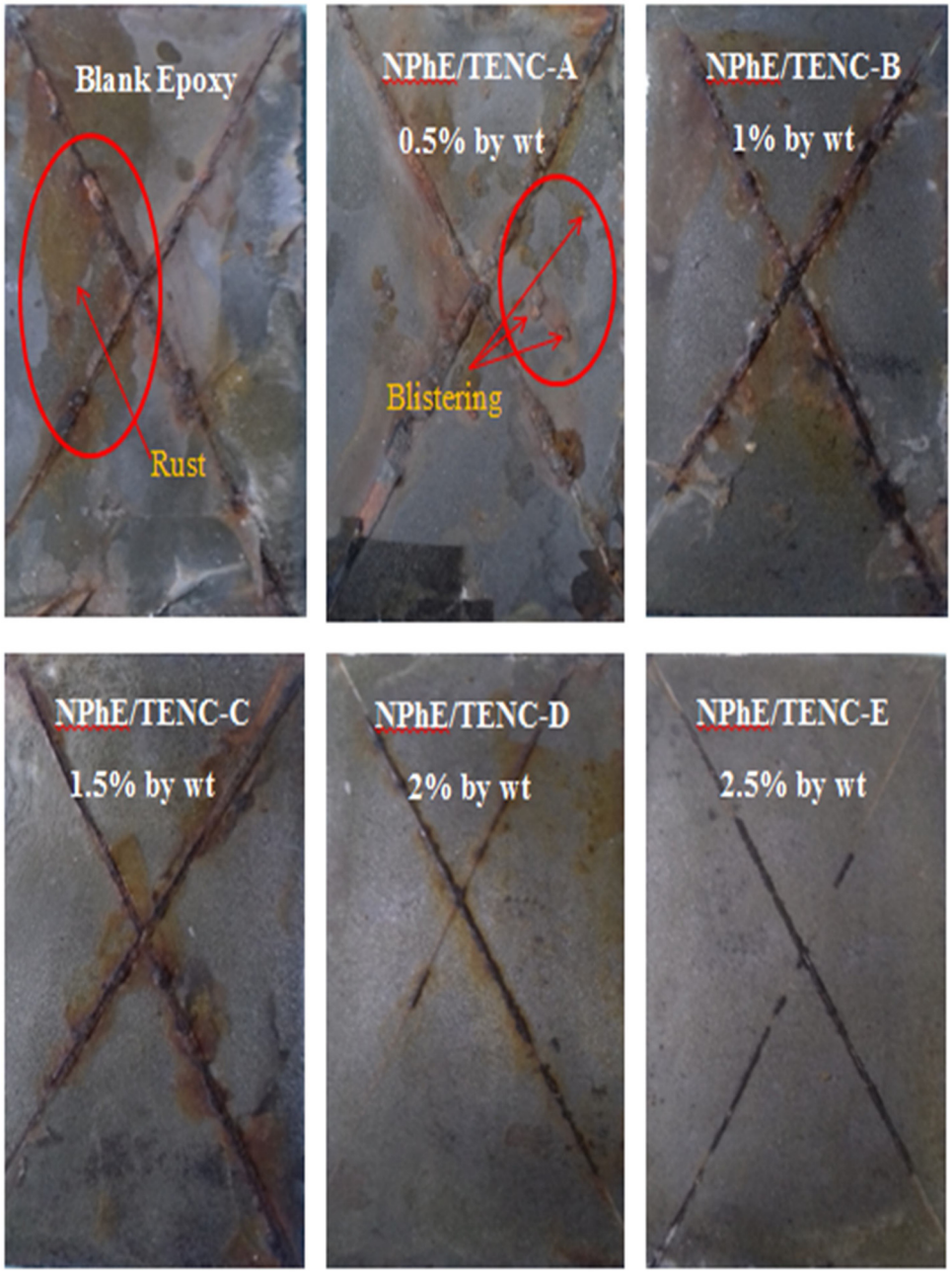

Fig. 5. Salt spray test for the investigated unmodified and various modified NPhE/TNC epoxy coated films after direct exposure to 5% NaCl solution for 500 h at 35 °C.

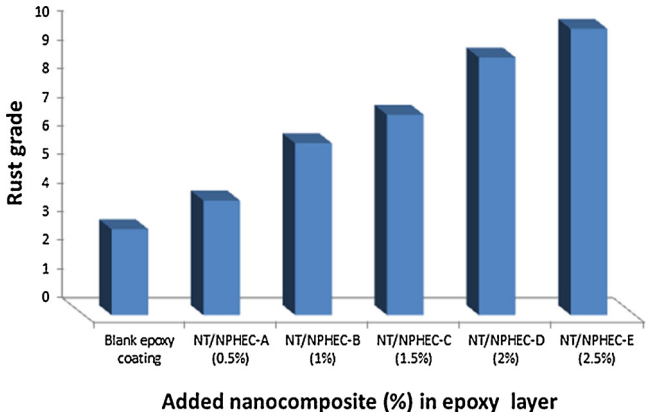

Fig. 6. The change in the rust grade values as a function of corrosion protection by adding NPhE/TNC with different concentrations in epoxy coating against unmodified epoxy after direct exposure to salt spray fog.

Where d is the distance where it is expected that no failure will occur by the dropped weight, g is the gravity wheel = 9.8 and m is the mass of cylindrical weight dropped on indenter.

2.9. Chemical resistance behavior

The chemical resistance performance test was performed according to ASTM D1308-02e1 to determine the influence of chemicals on blank and surface-modified NPhE/TNC epoxy coated films, producing changes in the coating surface, such as gloss alteration, color deterioration, swelling, blistering, softening and adhesion loss. In this investigation, immersion test was available in which coated specimens were immersed in the reagent. The coated specimens were immersed for 60 min, then washed by distilled water, cleaned by naphtha and detergent, and finally rinsed in deionized water. Drying with a towel and assessing after 24 h at room temperature and 55% relative humidity had been done utilizing the following rating levels: Level 0 - No change detected; Level 1 – Little change in gloss or color; Level 2 - Little smearing or surface etching; Level 3 - Swelling, pitting, cratering, or coating erosion and complete deterioration was recognized.

3. Results and discussion

3.1. Formulation mechanism of nonylphenol ethoxylate/TiO_2 epoxy nanocomposite (NPhE/TENC) coating

The formulation mechanism of NPhE/TENC coating was summarized in Scheme 1. Epoxy resin-based on diglycidyl ether of bisphenol-A (DGEBA) was used as a binder for all constituents of the investigated coating. Cyclohexanone was added as a solvent for the full-dispersion of TNPs with the NPhE to form homogeneous emulsion to be suitable for epoxy modification. NPhE was incorporated as a surfactant and pigment dispersing agent for the TNPs. NPhE/TNC paste was added to the epoxy coating to form the hybrid epoxy nanocomposite as a promoter for coating properties. Then, the xylene solvent was utilized as a viscosity controller for the coating emulsion. The neat epoxy coating was prepared without the incorporation of NPhE/TNP modifier. Isopropyl alcohol was employed as a modifier for enhancing the coating polarity. Ethylene glycol was added as a leveling material for the wet coating layer to modify the induction period of the coating. The coating flexibility was modified by using DOP as a plasticizer. Ancamine 1734 was used as a hardener for full curing and establishing perfect three-dimensional networks with the epoxy resin.

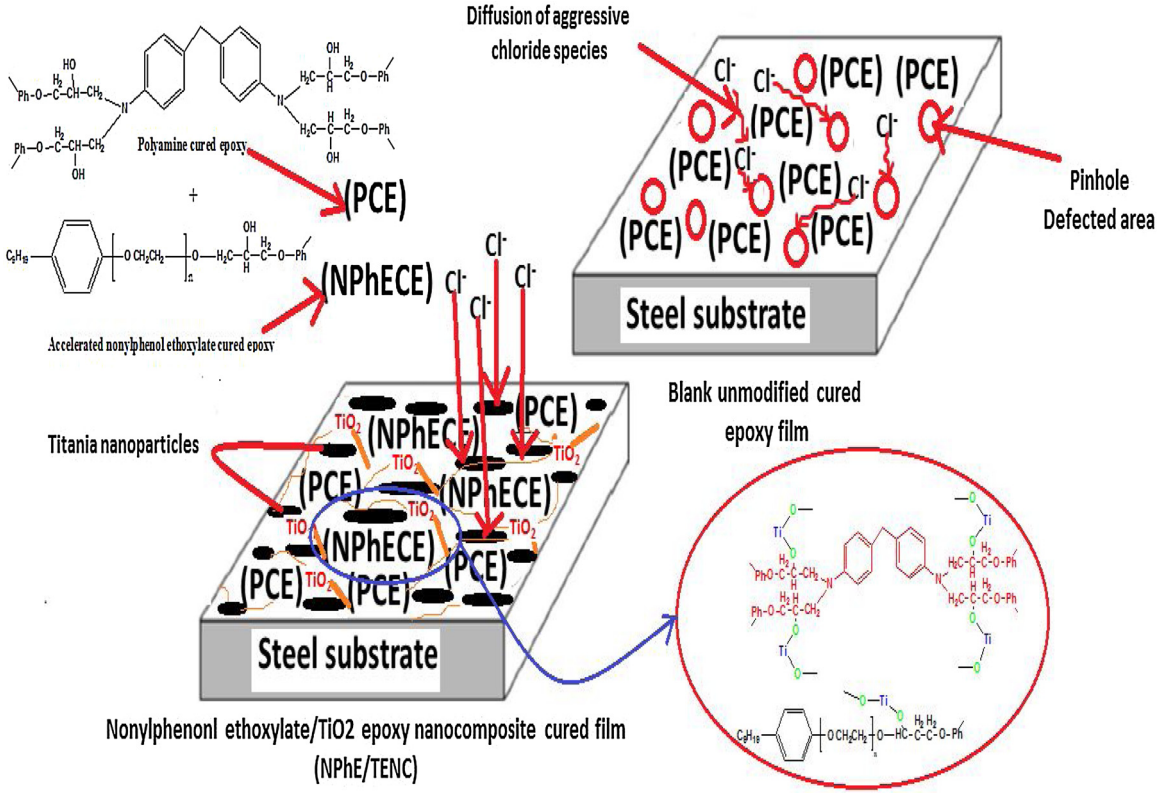

Fig. 7. The suggested corrosion mitigation mechanism of the surface-modified NPhE/TNC epoxy coating applied on C-steel substrate against unmodified conventional epoxy.

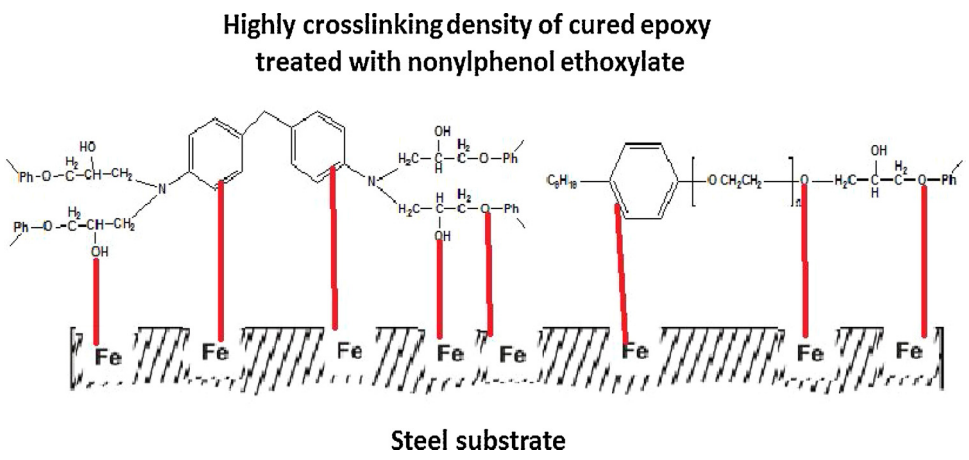

Fig. 8. Sketch illustrates the plastic adherent film formed due to the highly cross-linking density of modified NPhE epoxy coating.

3.2. Physicochemical characterization of TNPs

3.2.1. XRD analysis of TNPs

XRD patterns of the synthesized TNPs examined the phase identification of these particles and revealed the presence of mixed crystalline phases of tetragonal Anatase (65%) and tetragonal Rutile (35%) in the nanodimentions as shown in Fig. 1. The diffraction peaks illustrated in Fig. 1 were more intense and narrow, affirming the actual crystalline nature of the nano-sized TiO_2 grains.

3.2.2. TEM and SEM characterizations of TNPs

Visual inspection for the TEM images of TNPs displays the morphology of the nanoparticles as shown in Fig. 2. According to Fig. 2, it can be observed that TNPs are with lamellar shape in nanodimentions and the white bar present in the left bottom corner is a 50 nm-length reference for the TEM micrograph. The characteristic SEM micrograph as shown in Fig. 3 revealed that the TNPs have flaky-like shaped grains in which arranged in overlapping plates. Also, the SEM image affirmed the nano-scale of the used TNPs.

3.3. FT-IR spectra

The FT-IR spectra displayed a broad peak at 3458 cm^{-1} which is appointed to O—H stretching of cured epoxy [17,18]. The peaks at 3329 and 3144 cm^{-1} revealed the presence of primary amine N—H bond that attributed to Ancamine 1734 curing agent, but these peaks disppeared in Fig. 4 (b, c) referring to the cross-linking of all amino-groups. The peaks appeared in a range of 2966–2896 cm^{-1} were attributed to both asymmetric and symmetric stretching of methylene group ($-CH_2-$) [19,20]. The appearance of additional peaks at 1567 cm^{-1} and 1120 cm^{-1} was attribued to N—H bending and C—N stretching, respectively, confirming the condensation reaction between the $-NH_2$ group of Polyamine curing agent and the epoxide group of epoxy resin (DGEBA) [21]. The FT-IR spectra of nonylphenol ethoxylate/TiO_2 hybrid nanocomposite (NPhE/TNC) as illustrated in Fig. 4a, showed the appearance of new stretching peaks due to Ti–O (434, 485, and 829 cm^{-1}), O–Ti–O (692 cm^{-1}) and Ti—O—C (1180 and 1040 cm^{-1}) bonds. Also, these peaks are observed in the spectra of NPhE/TENC coating as shown in Fig. 4c. Furthermore, the shifts in —OH from 3424 cm^{-1} (epoxy) to 3423 cm^{-1} (epoxy-TiO_2 sol) and epoxide bands (from 910 (epoxy) to 917 cm^{-1} (epoxy–TiO_2 sol), revealing the condensation reactions of TNPs via epoxy resin [14]. Thus, the incorporation of TNPs in epoxy led to the formation of new O–Ti–O linkage, connecting the inorganic components with the organic epoxy phase. The peak records at 1489 cm^{-1} revealed the presence of —C═C— of aromatic rings of epoxy resin and NPhE. In addition, some signals appeared in the range of 1295–1182 cm^{-1}, indicating the presence of aliphatic chains [18]. The disappearance of peaks at 971, 917 and 775 cm^{-1} presented in Fig. 4a, which are characteristic to the terminal oxirane groups of epoxy, confirmed the cross-linking of epoxy resin [22]. The peaks of secondary O—H groups of cured epoxy at 972 cm^{-1} are disappeared due to the formation of C—O—Ti linkage [14] as displayed in Fig. 4c.

3.4. Anticorrosion behavior of the studied epoxy coated films

3.4.1. Accelerated corrosion test (Salt spray fog)

Accelerated corrosion test was performed to evaluate the coating degradation due to the presence of pores and crevices in the coated film [18]. Therefore, the anti-corrosion behavior was also investigated to clarify the influence of the employed NPhE/TNC on the protective performance of epoxy coating when compared with the unmodified epoxy (neat coating). The salt spray results after 500 h exposure to aggressive 5% NaCl medium were reported in Table 1 and presented in Fig. 5. The coating degradation after exposure to the aggressive atmosphere was observed for the blank epoxy coating (neat epoxy). For evaluation of the blistering size and frequency, adhesion class, softening, and the rust grade, a visual comparsion of photographic images with respect to reference standard photographs were performed. The data displayed that blank epoxy coating showed the existence of blisters at #3 size and medium dense frequency, rust grade (3), cured film softening and adhesion class (1B). Furthermore, corrosive brown products of iron hydroxides were detected on the coating surface, confriming the drastic chemical changes occured for blank epoxy coating [23]. In this case, the aggressive species such as water and chlorides will transfer through tortuous paths of the blank epoxy coated panel to reach the substrate surface [24]. As shown in Fig. 5, it was observed that the amounts of rust and blistering spread over the coating surface were diminished with increasing the loading level (%) by weight of NPhE/TNC through the cured epoxy coated layer. The visual photographic results for the NPhE/TENC-E coated film (surface-modified 2.5% NPhE/TNC modifier) showed the absence of blisters at #8 size with few frequency, no softening observed in the cured coating layer, the best corrosion mitigation performance at rust degree of 10, and perfect cross-cut adhesion of 5B grade. The blistering size is classified from #8 to #3, where #8 refers to no blistering and #3 exemplifies the largest blister size. The frequency of blistering is betokened by Few, Medium, Medium dense and Dense. Rust grade 10, refers to no rusting or less than 0.01% of surface rusted; rust grade 0 indicates approximately 100% of surface rusted [25]. This indicated that the maximum protective behavior was reached for NPhE/TENC-E coating. The protective behavior of the surface-treated epoxy nanocomposite coated layers with the NPhE/TNC paste against unmodified epoxy as a function of the rust grade was shown in Fig. 6.

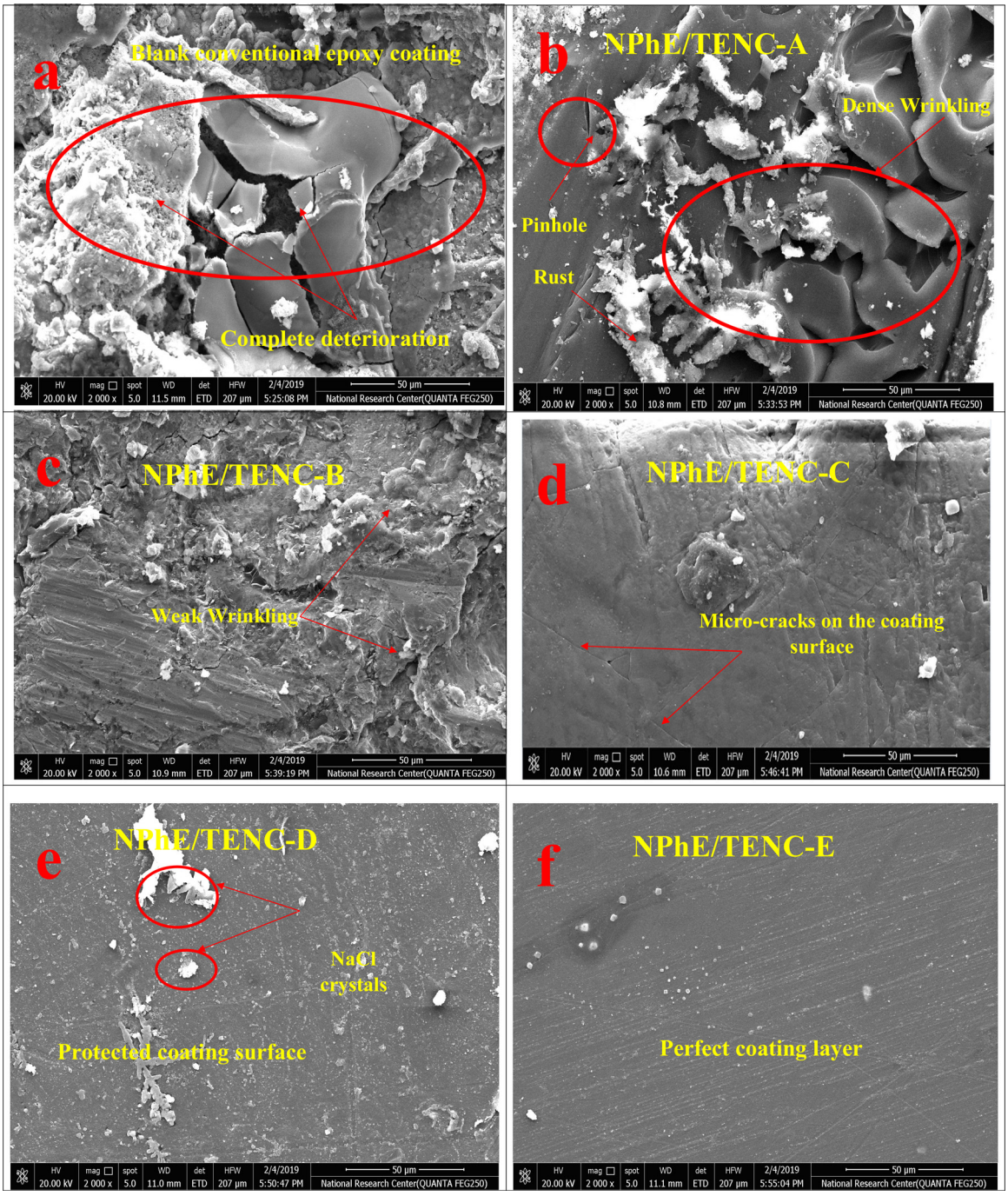

Fig. 9. SEM micrographs for a) unmodified epoxy, b) NPhE/TENC –A, c) NPhE/TENC-B, d) NPhE/TENC-C, e) NPhE/TENC-D and f) NPhE/TENC-E coating layers after direct exposure for salt spray fog for 500 h.

This reinforcement in the protective performance was assigned to the complete dispersion of NPhE/TNC particles via the epoxy vehicle matrix as a pigment which hindered the propagation of the aggressive salt spray fog via the coated layer, thereby enhancing the chemical bonding density and establishing an efficient protective barrier. Also, the presence of well-dispersed nanocomposite molecules led to the formation of Ti—O, Ti—O—C and O—Ti—O interconnections (inorganic phases) with epoxy (DGEBPA) and formed dense hybrid structure of polyamine cured DGEBPA-TiO_2 and NPhE-TiO_2 nanocomposites as shown in Scheme 1. This performance made TNPs absorb more epoxy binder on their surfaces and boost the coating film density, thereby diminishing the transmission ways for the aggressive fog (NaCl solution vapors) to penetrate the coating layer and reduce the steel corrosion [26–28] as illustrated in the anti-corrosion mechanism as shown in Fig. 7. The synergistic corrosion mitigation behavior of the surface-modified NPhE/TNC epoxy coating could be summarized in the following points: I). The prominent protective performance distinguished by the adsorption of aromatic rings π- electrons of DGEBPA and the oxygen atoms lone pair of NPhE on the C-steel substrate. Epoxy vehicle donating centers establish an adherent plastic layer with vacant orbitals of the steel substrate. The adhesion strength of the formed layer is enhanced in case of surface-modified NPhE/TNC epoxy coating owing to increasing the chemical bonding density (donor/acceptor interactions) reinforcing the adhesion with C-steel substrate in the mechanism offered in Fig. 8. The formed adherent layer can reduce the transmittance of the corrosive species to the C-steel substrate [29,30]. II) The

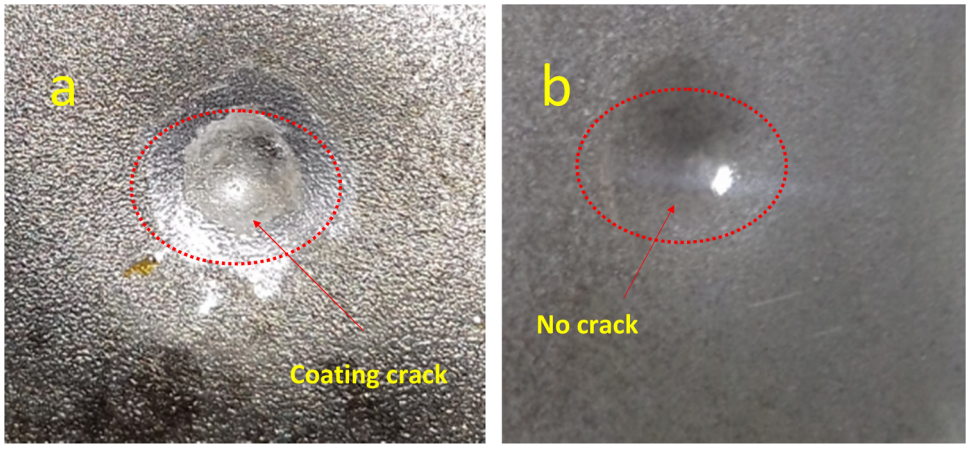

Fig. 10. Impact test for a) unmodified epoxy and b) NPhE/TENC-E coating layers.

Table 2
Chemical durability immersion test (Acid and alkali resistances) data for unmodified and modified NPhE/TNC epoxy coated films.

Coating code	Acid resistance (B: Nonvolatile liquid)			Alkali immovability (B) Sodium hydroxide (40%)
	Sulfuric acid (96%)	Nitric acid (70%)	Hydrochloric acid (37%)	
Blank epoxy coating	3	3	3	3
NPhE/TENC-A	3	3	2	2
NPhE/TENC-B	2	1	2	1
NPhE/TENC-C	1	0	1	0
NPhE/TENC-D	0	0	0	0
NPhE/TENC-E	0	0	0	0

existence of polar groups induces the robust electrostatic physical bonding between the steel substrate and epoxy film modified with NPhE, forming strong adherent film. III) The formed coating barrier by the cured modified epoxy nanocomposite coatings could be attributed to the well-dispersion of TNPs in which the interface interactions of the established Ti—O, Ti—O—C and O—Ti—O cluster networks with epoxy matrix were enhanced. This behavior reinforced the inter-coat adhesion, prevented agglomeration and upholded the surface protection [14]. The formed physical barrier prohibited the epoxy swelling, blistering and cracking due to preventing the transport of corrosive atmosphere to the steel substrate [1,30]. Also, the addition of fabricated NPhE/TNC modifier to epoxy enhanced the coating film hardness and resistance owing to enhancing the chemical interactions and reinforcing the cross-linking density (established due to the presence of titania cluster networks), thereby reinforcing the film hardness [28] as shown in Fig. 8. The epoxy coating hydrophobicity was enhanced due to increasing the cross-linking density between NPhE and epoxy terminals, thereby reducing the wettability of the corrosive environment. IV) The adhesion strength of the epoxy coating film relied on the hydrogen bonding interactions formed between the polar moieties of DGEBPA-NPhE system and the receptor sites of the C-steel substrate. In addition, the transport of H_2O molecules to epoxy/substrate interface in case of the neat coating occurs via the dispersion into pinholes and voids progressed over the coating layer [31]. V) The enhanced adhesion property observed for surface-treated NPhE/TNC epoxy coating can be attributed to the high compatibility between the fully-dispersed TNPs with metal complex molecules which occupy voids and pinholes dispersed over the coated film and work as bridges (Ti—O, Ti—O—C and O—Ti—O) in the interconnected epoxy matrix. That led to lowering the total free volumes and reinforcing the cured film cross-linking density. Thereafter, the cured layer has diminished segmental chain movements and enhanced stiffness [14,18]. Then, NPhE/TNC molecules prohibit the formation of pores through the epoxy layer and prevent the transmittance ways of aggressive salt spray fog to the coating/substrate interface. In case of unmodified conventional epoxy, the presence of water molecules induces the electrochemical reactions beneath the coating layers and the cathodic reactions resulted in the formation of OH^- anions. Then, the interaction between OH^- anions and Na^+ cations present in aggressive medium is made to establish NaOH molecules (strong alkaline agent) which is responsible for increasing the pH under the coating film then, coating delamination (bond destruction) occurs [32–34]. The enhancement in coating hydrophobicity due to the presence of NPhE/TNC modifier prevents the penetration of salt spray fog via the coating film then, supports the growth of the inorganic –O–Ti–O– and Ti–O–C nanophases. These nanophases create a well cross-linked network of the DGEBPA–TiO_2 hybrid nanocomposite sol and inhibit the coating film deterioration [35].

3.4.2. SEM morphology investigation

The surface morphology of blank (unmodified) epoxy and NPhE/TENC coated steel specimens were checked by SEM micrographs as shown in Fig. 9 to study the effect of direct exposure to aggressive salt spray fog on the coating surface characteristics. Fig. 9a showed the SEM image of blank epoxy coated steel panel in which complete deterioration (rust, wrinkling, and film cracking) in the epoxy coating surface was shown due to corrosion. For NPhE/TENC-A coated specimen (modified 0.5% NPhE/TNC), there are some rusted areas, dense wrinkling and some pinholes were progressed via the coating surface after exposure to the aggressive fog under the same conditions as shown in Fig. 9b. For NPhE/TENC-B coated film (modified 1% NPhE/TNC), weak wrinkling and the roughened surface was observed above the coating layer and localized nearby the top coating surface as displayed in Fig. 9c. In case of NPhE/TENC-D coated film (modified 1.5% NPhE/TNC), few micro-cracks were established over the surface of the coating layer as displayed in Fig. 9d. According to SEM micrographs, the coating delamination was clearly observed in case of blank epoxy and NPhE/TENC-A coated films as shown in Fig. 9 (a, b), due to the pH enhancement under the coating layer resulting from the formation of NaOH molecules produced by the electrochemical reactions beneath the coating. Also, this behavior could be attributed to the presence of permeation sites for the corrosive atmosphere to transfer through the coating layer. Then, the corrosion process was enhanced in addition to permitting the ingress of wrinkling. With increasing the concentration of NPhE/TNC modifier through the coating film, there was an improvement in the protective performance of epoxy coating as illustrated in Fig. 9 (c, d). The multi-protective behavior was observed for NPhE/TENC-D (modified 2% NPhE/TNC) and NPhE/TENC-E (modified 2.5% NPhE/TNC) coated films as shown in Fig. 9 (d, e) in which no any

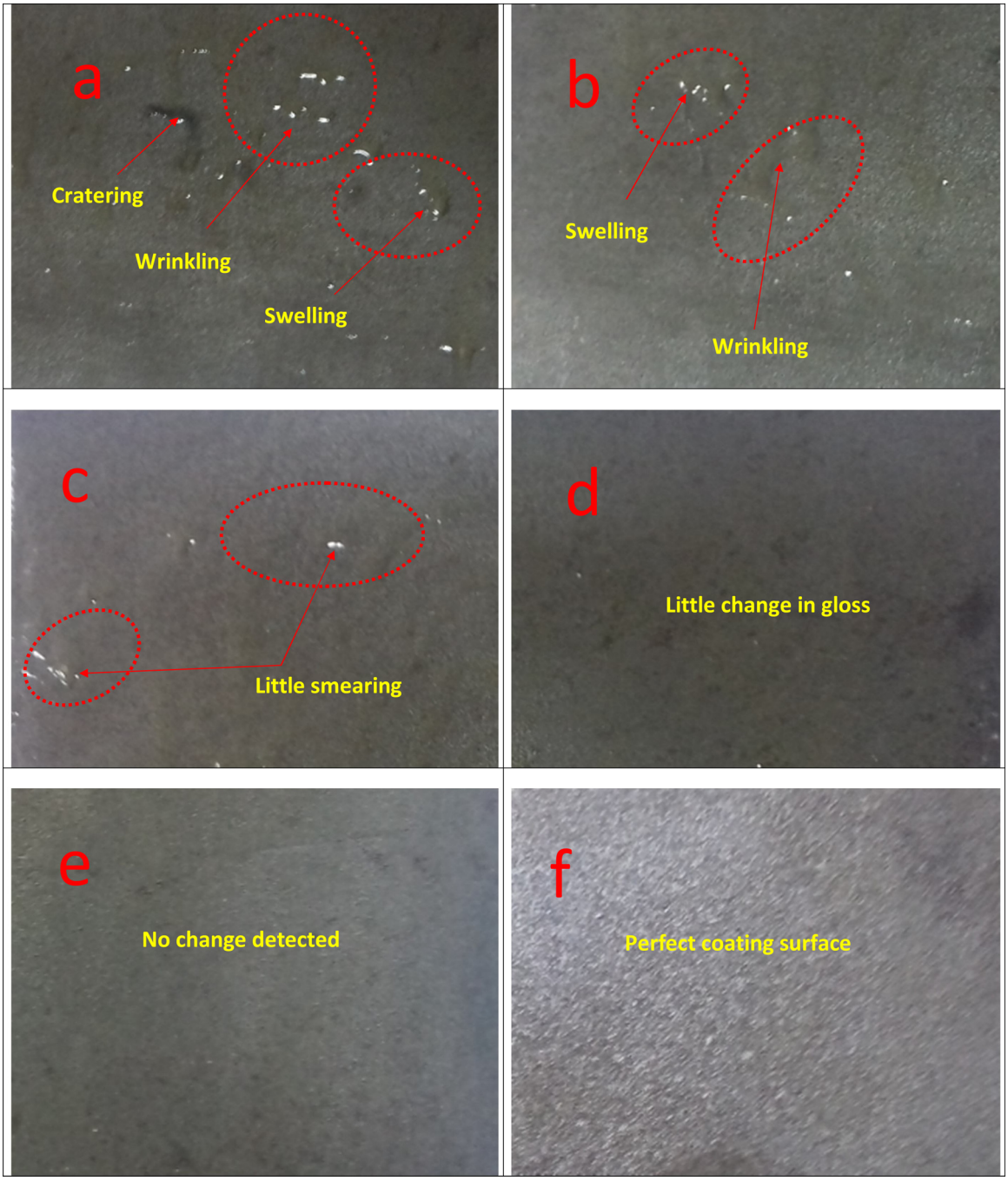

Fig. 11. Photographic images for a) unmodified epoxy, b) NPhE/TENC –A, c) NPhE/TENC-B, d) NPhE/TENC-C, e) NPhE/TENC-D and NPhE/TENC-E coated films after direct immersion in strong acids and alkali.

pores, rust, wrinkling or micro-cracks across the coating layer were detected. This performance could be assigned to the higher concentration of well-dispersed NPhE/TNC modifier particles with the epoxy coating, establishing a barrier of overlapping platelets. Then, this behavior increased the cross-linking density of the cured coating layer on the C-steel surface due to the formation of dense titania interconnections with epoxy and NPhE (DGEBA—O—Ti— and NPhE—O—Ti—) [36]. In addition, the interface interactions between the polar terminals of epoxy vehicle matrix and the dispersed particles were enhanced. Then, the inter-coating adhesion and the coating layer hardness were promoted causing a reduction in the steel corrosion [37,38]. The tiny size of TNPs permitted their transfusion into ultra-small capillaries through the coating layer, thereby producing a more compatible film. The enhancement in the cross-linking density reinforced the epoxy coating hydrophobicity and diminished the wettability and degradable effect of corrosive the salt spray fog.

3.5. Impact (resistance to rapid deformation) test

In this section, the resistance to rapid deformation (impact) test was performed to investigate the load distribution of the employed modified NPhE/TNC epoxy coating systems against neat epoxy as shown in Fig. 10. The results of direct impact were reported as; Blank epoxy coating (25) < NPhE/TENC-A (29) < NPhE/TENC-B (33) < NPhE/TENC-C (41) < NPhE/TENC-D (49) < NPhE/TENC-E (51), in which the impact resistance value was enhanced with increasing the

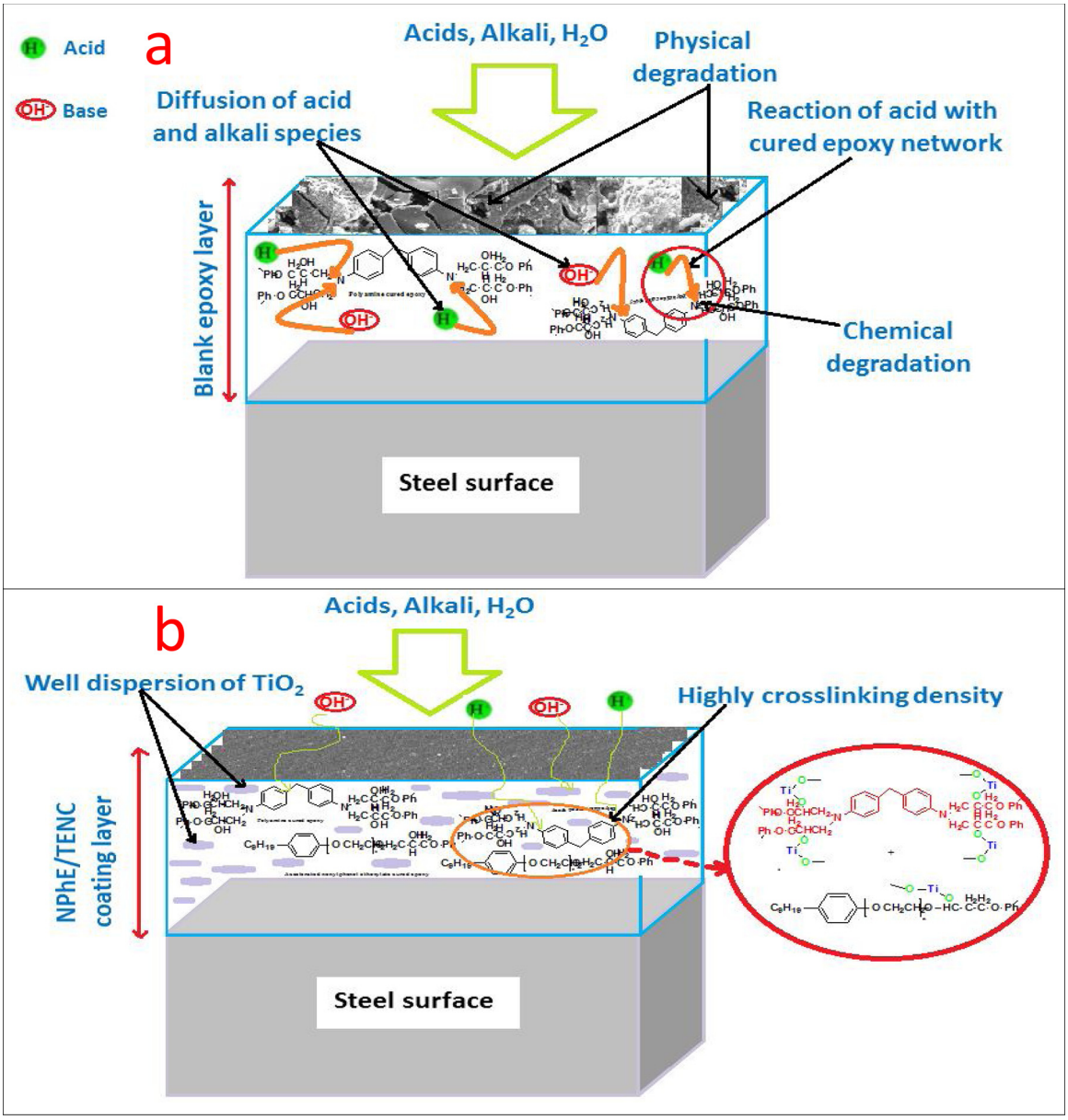

Fig. 12. The expected chemical resistance mechanisms for a) Unmodified epoxy, b) Modified NPhE/TENC-E coated film after direct immersion in strong acids and alkali for 60 min.

concentration of nanocomposite modifier through the coating film. As illustrated in Fig. 10a, failure (epoxy fracture) was observed for the conventional epoxy coating layer after exposure to the direct impact and the coating film achieved the least resistance value at 25 J. This performance could be assigned to the mechanical stress established via the spreading free volumes (voids and pinholes) on the coating surface, thereby generating epoxy fractures and complete coating deterioration. The efficient resistance to rapid deformation was observed for NPhE/TENC-E coated film as shown in Fig. 10b and recorded at 51 J. This behavior could be attributed to the enhancement in the interface surface interactions between the NPhE/TNC molecules and epoxy resin matrix. This led to promoting the bonding between the epoxy and NPhE polar moieties and TNPs (DGEBA−O−Ti− and NPhE−O−Ti− linkages) at the C-steel surface, thereby consolidating the internal coating adhesion, restricting the coating chain mobility and promoting the crosslinking density [39,40]. This behavior decreased the microvoids via the coating layer and diminished the mechanical stress and progress of any cracks or loss of coating adhesion [41].

3.6. Chemical immovability performance

The chemical immovability is a vital test for evaluating the protective coating layer resistance to acids and alkali harsh attack [42]. The acid-durability of an epoxy coating is a function of all its constituents in addition to surface preparation (polishing), application style, and curing conditions [43]. According to the results reported in Table 2, it is found that blank epoxy coating was exposed to a significant chemical deterioration (level 3) after direct immersion in various severe media such as sulfuric acid 96%, nitric acid 70%, hydrochloric acid 37% and sodium hydroxide 40%. The coating film degradation showed swelling, wrinkling and cratering as shown in Fig. 11a. Two types of degradation mechanisms were shown for the blank epoxy coated film. Firstly, the physical degradation was observed in which represented in the diffusion of acid and alkali species to enable the connection between the propagated species, coating, and ultimately the underlying surface. This led to produce coating layer swelling, cratering, wrinkling and mechanical damage. The Physical degradation was progressed due to the spreading of free volume spaces (voids and

pinholes) via the epoxy resin matrix, then, penetrant molecules (acids and alkali) could "jump" from one pinhole to another. The penetrant molecules could present in an unbound or bound states in voids, thereafter the cohesive forces connected the penetrant molecules to the epoxy coating network as shown in Fig. 11a. For the dissociated acids, the protons and anions shifted with each other to preserve charge neutrality [44,45]. In the case of alkali media such as NaOH, a vigorous alkaline agent and in the presence of water molecules, the pH under the coating layer increased and caused the coating delamination (destruction of adhesion bonds). Secondly, the chemical degradation was observed and progressed inside the coating film due to the acid-hydrolysis and chemical oxidation reactions initiated in touch with the acid environment and could cause epoxy resin bond breaking and functional groups reactivity like alcohol groups conversion to ketones. In the case of NPhE/TENC-A coated film, the physical and chemical degradations were observed also after the immersion process but the swelling and wrinkling volumes were lower than the detected defects in blank neat epoxy as shown in Fig. 11b. This behavior could be assigned to supporting the cross-linking density by the O—Ti—O and C—O—Ti interconnections with epoxy and NPhE. With increasing the loading weight percent (%) of NPhE/TNC modifier through the coated film, an incremental improvement in the chemical resistance and film rigidity was observed because of the increasing in cross-linking density and increasing in O—Ti—O and C—O—Ti nanoscale linkages with epoxy and NPhE as shown in Fig. 11 (c, d). This cross-linking decreased the epoxy network segmental mobility and reduced the generation of pinholes over the coating film, thereby limiting the diffusion of the acids and alkali molecules via the epoxy layer [46]. Perfect chemical immovability (level 0) and film rigidity are observed in case of NPhE/TENC-D and NPhE/TENC-E coated steel panels as shown in Fig. 11 (e, f) and reported in Table 2. This performance could be assigned to the regular dispersion and complete compatibility of NPhE and TiO_2 nanoparticles with the epoxy coating, generating a barrier of the overlapping platelets and an enhancement in cross-linking density of the cured film on the C-steel surface. This behavior enhanced the coating film rigidity due to formation of O—Ti—O and C—O—Ti nanoscale linkages with DGEBPA, thereby producing more compacted and hydrophobic networks and preventing the effect of protons and anions of the dissociated acids. These employed hydrophobic networks acted as effective barriers to prohibit the diffusion of acid and alkali species through the coating layer [47]. The predicted chemical durability mechanism of NPhE/TENC-E coating against unmodified epoxy was shown in Fig. 12 (a, b)

4. Conclusions

Nonylphenol ethoxylate/TiO_2 nanocomposite modifier was prepared and incorporated to epoxy with different loading levels (%) by weight to enhance the corrosion mitigation performance, impact resistance and chemical durability of cured coating layer. The protective behavior of the coated films was investigated using salt spray accelerated corrosion test. The visual photographic results showed the complete degradation of conventional epoxy film. The perfect anticorrosion performance was exhibited for NPhE/TENC-E (2.5% NPhE/TNC). SEM investigation confirmed the corrosion mitigation behavior of the surface-modified NPhE/TNC epoxy coating layers. Resistance to rapid deformation (impact) test demonstrated the toughened and compacted epoxy coating layer treated with NPhE/TNC modifier. Perfect chemical immovability to strong acid and alkali solutions (level 0) and film rigidity were observed in case of NPhE/TENC-D and NPhE/TENC-E coated steel panels. The enhancement in epoxy coating resistance properties could be assigned to the increasing in O—Ti—O and C—O—Ti nanoscale linkages with epoxy and NPhE in which a growing in three-dimensional networks density was made, thereby leading to the formation of strong barrier film, restricting the chain mobility via the coating layer and improving layer rigidity.

Acknowledgment

I would like to extend my sincere thanks, appreciation, and gratitude to EPRI and Faculty of Science, Zagazig University for their technical, financial and scientific support.

References

[1] Sharifi Golru, M.M. Attar, B. Ramezanzadeh, Studying the influence of nano-Al_2O_3 particles on the corrosion performance and hydrolytic degradation resistance of an epoxy/polyamide coating on AA-1050, Prog. Org. Coat. 77 (2014) 1391–1399.
[2] B. Ramezanzadeh, Z. Haeri, M. Ramezanzadeh, A facile route of making silica nanoparticles-covered graphene oxide nanohybrids (SiO2-GO); fabrication of SiO2-GO/epoxy composite coating with superior barrier and corrosion protection performance, Chem. Eng. J. 303 (2016) 511–528.
[3] Amir H. Navarchian, Mehrnaz Joulazadeh, Fariba Karimi, Investigation of corrosion protection performance of epoxy coatings modified by polyaniline/clay nanocomposites on steel surfaces, Prog. Org. Coat. 77 (2014) 347–353.
[4] Tuan Anh Nguyen, The Huyen Nguyen, Thien Vuong Nguyen, Hoang Thai, Xianming Shi, Effect of nanoparticles on the thermal and mechanical properties of epoxy coatings, J. Nanosci. Nanotech. 15 (2016) 1–8.
[5] M. Nematollahi, M. Heidarian, M. Peikari, S.M. Kassiriha, N. Arianpouya, M. Esmaeilpour, Comparison between the effect of nano glass flake and montmorillonite organoclay on corrosion performance of the epoxy coating, Corros. Sci. 52 (2010) 1809–1817.
[6] B. Ramezanzadeh, M.M. Attar, Studying the corrosion resistance and hydrolytic degradation of an epoxy coating containing ZnO nanoparticles, Mater. Chem. Phys. 130 (2011) 1208–1219.
[7] S. Niroumandrad, M. Rostami, B. Ramezanzadeh, Effects of combined surface treatments of aluminum nanoparticle on its corrosion resistance before and after inclusion into an epoxy coating, Prog. Org. Coat. 101 (2016) 486–501.
[8] A. Ghanbari, M.M. Attar, A study on the anticorrosion performance of epoxy nanocomposite coatings containing epoxy-silane treated nano-silica on mild steel substrate, J. Ind. Eng. Chem. 23 (2015) 145–153.
[9] A. Hartwig, M. Sebald, D. Putz, L. Aberle, Preparation, characterization, and properties of nanocomposites based on epoxy resins – an overview, Macromol. Symp. 221 (2005) 127–136.
[10] M. Conradi, A. Kocijan, D. Kek-Merl, M. Zorko, I. Verpoest, Mechanical and anticorrosion properties of nano silica-filled epoxy resin composite coatings, Appl. Surf. Sci. 292 (2014) 432–437.
[11] Hongwei Shi, Fuchun Liu, Lihong Yang, Enhou Han, Characterization of the protective performance of epoxy reinforced with nanometer-sized TiO_2 and SiO_2, Prog. Org. Coat. 62 (2008) 359–368.
[12] Min Zhi Rong, Ming Qiu Zhang, Microstructure and tribological behavior of polymeric nanocomposites, J. Ind. Lub. Tribol. 53 (2001) 72–77.
[13] C.B. Ng, L.S. Schadler, R.W. Siegel, Synthesis and mechanical properties of TiO_2-epoxy nanocomposites, Nanostruct. Mater. 12 (1999) 507–510.
[14] Anujit Ghosal, Sharif Ahmad, High-performance anti-corrosive epoxy–titania hybrid nanocomposite coatings, New J. Chem. 41 (2017) 4599–4610.
[15] Mehdi Derradji, Noureddine Ramdani, Jun Wang TongZhang, Lin-dan Gong, Xiaodong Xu, Zai-wen Lin, Abdelkhalek Henniche, H.K.S. Rahoma, Wen-bin Liu, Effect of silane surface-modified titania nanoparticles on the thermal, mechanical, and corrosion protective properties of a bisphenol-A based phthalonitrile resin, Prog. Org. Coat. 90 (2016) 34–43.
[16] M.A. Ahmed, Z.M. Abou-Gamra, H.A.A. Medien, M.A. Hamza, Effect of porphyrin on photocatalytic activity of TiO2 nanoparticles toward Rhodamine B photodegradation, J. Photochem. Photobiol. B, Biol. 176 (2017) 25–35.
[17] R.M. Silverstein, G.C. Bassler, T.C. Morrill, Spectrometric Identification of Organic Compounds, 4th ed., John Wiley and Sons, New York, NY, USA, 1981.
[18] M.I. Abdou, M.I. Ayad, A.S.M. Diab, I.A. Hassan, A.M. Fadl, Influence of surface-modified ilmenite/melamine-formaldehyde composite on the anti-corrosion and mechanical properties of conventional polyamine cured epoxy for internal coating of gas and oil transmission pipelines, Prog. Org. Coat. 113 (2017) 1–14.
[19] M. Jaisai, S. Baruah, J. Dutta, Paper modified with ZnO nanorods – antimicrobial studies, Beilstein J. Nanotechnol. 3 (2012) 684–691.
[20] F. Zafar, E. Sharmin, S. Ashraf, S. Ahmad, Studies on poly(styrene-co-maleic anhydride)-modified polyesteramide-based anticorrosive coatings synthesized from a sustainable resource, J. Appl. Polym. Sci. 92 (2004) 2538–2544.
[21] S. Ahmad, A. Gupta, E. Sharmin, M. Alam, S. Pandey, Synthesis, characterization and development of high-performance siloxane-modified epoxy paints, Prog. Org. Coat. 54 (2005) 248–255.
[22] S. Felahi, N. Chikhi, M. Bakar, Modification of epoxy resin with kaolin as a toughening agent, J. Appl. Polym. Sci. 82 (2001) 861–878.
[23] M. Nematollahi, M. Heidarian, M. Peikari, S.M. Kassiriha, N. Arianpouya, M. Esmaeilpour, Comparison between the effect of nanoglass flake and montmorillonite organoclay on corrosion performance of the epoxy coating, Corros. Sci. 52 (2010) 1809–1817.
[24] A.M. Fadl, M.I. Abdou, Doaa Laila, S.A. Sadeek, Application insights of Schiff base metal complex/SiO2 hybrid epoxy nanocomposite for steel surface coating: correlation the protective behavior and mechanical properties with material loading, Prog. Org. Coat. (2019) In press.
[25] O.A.G. Wahba, A.M. Hassan, A.M. Naser, A.M. Hanafi, Preparation and spectroscopic studies of some copper and nickel Schiff base complexes and their

applications as coloring pigments in the protective paints industry, Egypt. J. Chem. 60 (2017) 25–40.
[26] L.H. Yang, F.C. Liu, E.H. Han, Effects of P/B on the properties of anticorrosive coatings with different particle size, Prog. Org. Coat. 53 (2) (2005) 91–98.
[27] A. Kalendova, Effects of particle sizes and shapes of zinc metal on the properties of anticorrosive coatings, Prog. Org. Coat. 46 (4) (2003) 324–332.
[28] Hongwei Shi, Fuchun Liu, Enhou Han, Yinghua Wei, Effect of nano pigments on the corrosion resistance of alkyd coatings, J. Mater. Sci. Technol. 23 (4) (2007) 551–558.
[29] A.M. Fadl, A.M. Al-Sabagh, M.I. Abdou, M.A. Migahed, Method for preparation epoxy lotion from ilmenite ore to protect steel structures from corrosion, ARE Patent no. 27679 (2016).
[30] A.M. AlSabagh, M.I. Abdou, M.A. Migahed, S. AbdElwanees, A.M. Fadl, A. Deiab, Investigations using potentiodynamic polarization measurements, cure durability, ultraviolet immovability and abrasion resistance of polyamine cured ilmenite epoxy coating for oil and gas storage steel tanks in the petroleum sector, Egypt. J. Pet. 27 (2018) 415–425.
[31] B. Ramezanzadeh, A. Ahmadi, M. Mahdavian, Enhancement of the corrosion protection performance and cathodic delamination resistance of epoxy coating through the treatment of steel substrate by a novel nanometric sol-gel based silane composite film filled with functionalized grapheme oxides nanosheets, Corros. Sci. 109 (2016) 182–205.
[32] P.A. Sorenson, K. Dam-Johansen, C.E. Weinell, S. Kiil, Cathodic delamination: quantification of ionic transport rates along coating-steel interfaces, Prog. Org. Coat. 67 (2010) 107–115.
[33] M.I. Abdou, M.I. Ayad, A.S.M. Diab, I.A. Hassan, A.M. Fadl, Studying the corrosion mitigation behavior and chemical durability of $FeTiO_3$/melamine formaldehyde epoxy composite coating for steel internal lining applications, Prog. Org. Coat. 133 (2019) 325–339.
[34] M.I. Abdou, A.M. Fadl, Assessment of nano-FeTiO3/non crystalline silica cold galvanizing composite coating as a duplex corrosion guard system for steel electricity transmission towers in severe aggressive media, Constr. Build. Mater. 223 (2019) 705–723.
[35] C.S. Wu, In situ polymerization of titanium isopropoxide in polycarbolactone: properties and characterization of the hybrid nanocomposites, J. Appl. Polym. Sci. 92 (2004) 1749–1757.
[36] H. Wang, P. Xu, S. Meng, W. Zhong, W. Du, Q. Du, Poly(methyl methacrylate)/silica/titania ternary nanocomposites with greatly improved thermal and ultraviolet-shielding properties, Polym. Degrad. Stab. 91 (2006) 1455–1461.
[37] S. Momeni, W. Tillmann, M. Pohl, Composite cavitation resistant PVD coatings based on NiTi thin films, Mater. Design. 110 (2016) 830–838.
[38] M.A. Amin, Weight loss, polarization, electrochemical impedance spectroscopy, SEM and EDX studies of the corrosion inhibition of copper in aerated NaCl solutions, J. Appl. Electrochem. 36 (2) (2006) 215–226.
[39] S.K. Dhoke, R. Bhandari, A. Khanna, Effect of nano-ZnO addition on the silicone-modified alkyd-based waterborne coatings on its mechanical and heat-resistance properties, Prog. Org. Coat. 64 (2009) 39–46.
[40] B. Wetzel, F. Haupert, M. Qiu Zhang, Epoxy nanocomposites with high mechanical and tribological performance, Compos. Sci. Technol. 63 (2003) 2055–2067.
[41] B. De, N. Karak, Novel high performance tough hyperbranched epoxy by an $A_2 + B_3$ polycondensation reaction, J. Mater. Chem. A. 1 (2013) 348–353.
[42] C.H. Hare, Chemically induced degradation, J. Prot. Coat. Linings 16 (1999) 17–25.
[43] H.Q. Pham, M.J. Marks, Epoxy Resins in Ullmann's Encyclopedia of Industrial Chemistry, Wiley-VCH, 2005, pp. 155–244.
[44] M.H. Banna, J. Shiroko, J. Molgaard, Effects of two aqueous acidic solutions on polyester and bisphenol A epoxy vinyl ester resins, Mater. Sci. Eng.: A 528 (2011) 2137–2142.
[45] S.C. George, S. Thomas, Transport phenomena through polymeric systems, Prog. Poly. Sci. 26 (2001) 985–1017.
[46] Z.W. Wicks, F.N. Jones, Coatings in Kirk-Othmer Encyclopedia of Chemical Technology, John Wiley and Sons, 2013, pp. 1–88.
[47] Maryam Jouyandeh, Meisam Shabanian, Mahroo Khaleghi, Seyed Mohammad Reza Paranc, Samira Ghiyasi, Henri Vahabi, Krzysztof Formula, Debora Puglia, Mohammad Reza Saebg, Acid-aided epoxy-amine curing reaction as reflected in epoxy/Fe_3O_4 nanocomposites: chemistry, mechanism, and fracture behavior, Prog. Org. Coat. 125 (2018) 384–392.